10330 *Inorg. Chem.* **2010**, *49*, 10330–10337
DOI: 10.1021/ic101075g

Inorganic Chemistry
Article

Pathway from Chain to Dimer in Cu(I) Camphor Hydrazone Complexes

M. Fernanda N. N. Carvalho,*,† M. Teresa Duarte,† Tiago A. Fernandes,† Adelino M. Galvão,† and Ana M. Botelho do Rego‡

†*CQE, Complexo I, Instituto Superior Técnico, Technical University of Lisbon, Av. Rovisco Pais 1049-001 Lisboa, Portugal, and* ‡*Centro de Química-Física Molecular* (*CQFM*) *and Institute of Nanoscience and Nanotechnology* (*IN*), *Complexo Interdisciplinar, Instituto Superior Técnico, Technical University of Lisbon, Av. Rovisco Pais, 1049-001 Lisboa, Portugal*

Received May 27, 2010

The chemical reactivity, molecular structure, and surface characteristics of Cu(I) camphor hydrazone compounds indicate that exist a structural pathway for conversion of coordination polymers into dimers and vice versa. By X-ray diffraction analysis two polymorphic forms of the chain compound $[\{CuCl\}_2(Me_2NNC_{10}H_{14}O)]_n$ were identified that essentially differ in the structural arrangement and geometry of the non-linear copper atom. The characterization of the dimer complexes $[\{Cu(Me_2NNC_{10}H_{14}O)\}_2(\mu\text{-}X)_2]$ (X = Cl or Br) was also achieved by X-ray diffraction analysis showing the unusual arrangement of the camphor hydrazone ligands that occupy the same side of the molecule. Bond lengths and torsion angles show that one of the polymorphic forms is structurally close to the related dimer. The surface composition of the coordination polymers $[\{CuX\}_2(YNC_{10}H_{14}O)]_n$ (X = Cl, Y = NMe_2, NH_2; X = Br, Y = NH_2) and dimers $[\{Cu(Me_2NNC_{10}H_{14}O)\}_2(\mu\text{-}X)_2]$ (X = Cl or Br) studied by X-ray Photoelectron Spectroscopy corroborate the molecular properties and the reactivity trend.

Introduction

The polymer character of $[\{CuCl\}_2(Me_2NNC_{10}H_{14}O)]_n$[1] formed by two Cu(I) units with different structures and neighborhoods prompted the study of the chemical reactivity and surface properties of compounds $[\{CuX\}_2(YNC_{10}H_{14}O)]_n$ (X = Cl, Br; Y = NMe_2, NHMe, NH_2) for two main reasons: (i) research on the characteristics of coordination polymers is an area of current interest because of their hybrid nanomaterials[2] character with applications in catalysis,[3] biology, biomedicine (imaging and drug delivery)[4] and also because we found that (ii) two polymorphic forms of $[\{CuCl\}_2(Me_2NNC_{10}H_{14}O)]_n$ exist. Polymorphism is an important molecular characteristic to control functionality in materials[5] since it may induce different physical and chemical properties. Examples of polymorphism in coordination polymers are scarce in contrast to well documented examples in organic and organometallic compounds.[6] The study of the surfaces of Cu(I) camphor hydrazone compounds by X-ray Photoelectron Spectroscopy allows a first insight into properties that may scale up from molecules to materials.

Results and Discussion

Molecular Characterization and Reactivity. Two distinct forms of $[\{CuCl\}_2(Me_2NNC_{10}H_{14}O)]_n$ were identified by X-ray analysis: orange needle shaped crystals (**1a**) that crystallize in the monoclinic $P2_1$ space group (Figure 1a) and red cubic shaped crystals (**1a′**) that crystallize in the orthorhombic space group $P2_12_12_1$ (Figure 1b). Data from **1a** and **1a′**was collected at 150 K for an accurate comparison and to exclude the possibility of temperature driven polymorphism. Just slight differences were found in the parameters collected on **1a′** at room temperature (RT)[1] and at 150 K.

A systematic variation of the experimental conditions (temperature, reagent ratio, crystallization time) indicate concomitant crystallization of $[\{CuCl\}_2(Me_2NNC_{10}H_{14}O)]_n$ in the two polymorphic forms. However, crystals suitable for X-ray analysis are preferentially obtained in the red form **1a′**. The polymorphs display by IR frequencies (ν_{CO}: 1701, **1a**; 1691, **1a′**) that differ by about 10 cm^{-1} which is very convenient to distinguish them in the bulk.

The chain compound $[\{CuCl\}_2(Me_2NNC_{10}H_{14}O)]_n$ is formed by sequential linear (Cu1) and non-linear (Cu2) copper units. The Cu−Cl bond lengths at the linear units (Cu1) are similar in **1a** or **1a′** and just small differences exist in the Cl−Cu−Cl angles, that is, about 4° larger in **1a′**(178.45(2)° (Table 1).

*To whom correspondence should be addressed. E-mail: fcarvalho@ist.utl.pt.

(1) Carvalho, M. F. N. N.; Fernandes, T. A.; Galvão, A. M.; Krug von Nidda, H.-A.; Sampaio, M. A. P. *Inorg. Chim. Acta* **2010**, *363*, 71.
(2) Lin, W.; Rieter, W. J.; Taylor, K. M. L. *Angew. Chem., Int. Ed.* **2009**, *48*, 650–658.
(3) Wu, C.-D.; Li, L.; Shi, L. X. *Dalton Trans.* **2009**, 6790.
(4) Kim, J.; Lee, J. E.; Lee, S. H.; Yu, J. H.; Lee, J. H.; Park, T. G.; Hyeon, T. *Adv. Mater.* **2008**, *20*, 478, and references therein.
(5) *Polymorphism in Molecular Crystals*; Bernstein, J., Ed.; Oxford Science Publications: Oxford, U.K., 2006.
(6) Braga, D.; Maini, L.; Polito, M.; Scaccianoce, L.; Cojazzi, G.; Grepioni, F. *Coord. Chem. Rev.* **2001**, *216−217*, 225–248.

 Published on Web 10/13/2010

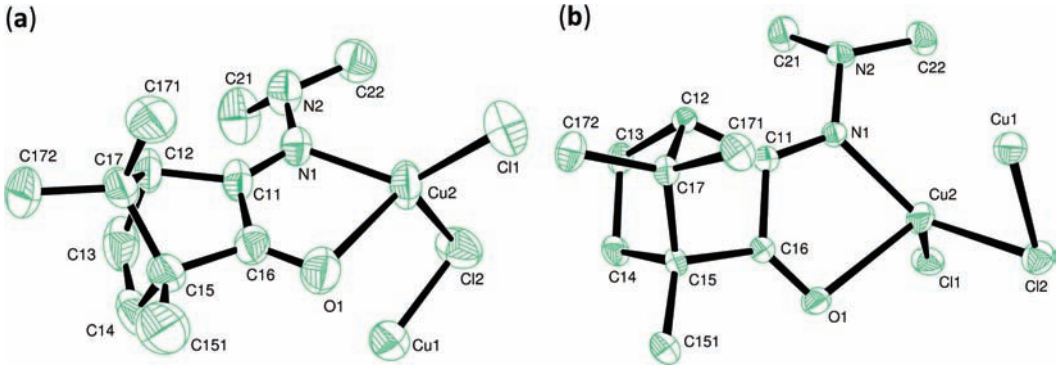

Figure 1. ORTEP drawing for $[\{CuCl\}_2(Me_2NNC_{10}H_{14}O)]_n$ showing labeling scheme: (a) **1a**; (b) **1a′**.

Table 1. Selected Bond Lengths and Angles for Complexes $[(CuCl)_2Me_2NNC_{10}H_{14}O)]_n$ (**1a**, **1a′**), $[\{Cu(Me_2NNC_{10}H_{14}O)\}_2(\mu\text{-Cl})_2]$ (**3a**), and $[\{Cu(Me_2NNC_{10}H_{14}O)\}_2(\mu\text{-Br})_2]$ (**4a**)[a]

	1a	**1a′**		(**3a**) X = Cl	(**4a**) X = Br
			Bond Lengths (Å)		
Cu1−Cu2	3.058(1)	2.944(1)	Cu1−Cu2	2.892(1)	2.856(2)
Cu2−Cl2	2.332(1)	2.322(1)	Cu1−X1	2.321(2)	2.419(2)
Cu2−Cl1	2.269(1)	2.287(1)	Cu1−X2	2.319(2)	2.445(2)
Cu1−Cl2	2.112(1)	2.114(1)	Cu2−X1	2.321(2)	2.441(2)
Cu1−Cl1#	2.114(1)[1]	2.116(1)	Cu2−X2	2.318(2)	2.409(2)
Cu2−N1	2.019(3)	2.012(1)	Cu1−N11	2.052(6)	2.079(8)
Cu2−O1	2.472(3)	2.375(1)	Cu1−O1	2.319(4)	2.303(6)
C1−N1	1.276(4)	1.293(2)	Cu2−N21	2.055(6)	2.102(8)
C2−O1	1.225(4)	1.213(2)	Cu2−O21	2.321(4)	2.275(7)
C2−C1	1.485(5)	1.497(2)	C11−N11	1.298(7)	1.30(1)
N1−N2	1.377(4)	1.389(2)	C12−O11	1.225(8)	1.21(1)
			C11−C12	1.487(9)	1.48(1)
			C22−N21	1.288(8)	1.30(1)
			C21−O21	1.224(7)	1.24(1)
			C21−C22	1.483(9)	1.48(1)
			N11−N12	1.336(7)	1.34(1)
			N21−N22	1.357(7)	1.33(1)
			Angles (deg)		
Cl1−Cu2−Cl2	111.64(5)	110.88(2)	Cu1−X1−Cu2	77.2(1)	72.0(1)
Cl2−Cu1−Cl1#	174.53(5)[1]	178.45(2)	Cu1−X2−Cu2	77.1(1)	72.1(1)
Cl1−Cu2−N1	127.7(1)	130.57(5)	X1−Cu1−X2	101.0(1)	106.3(1)
Cl2−Cu2−N1	114.5(1)	116.78(5)	X1−Cu2−X2	101.0(1)	106.7(1)
O1−Cu2−N1	76.7(1)	78.65(5)	X2−Cu1−N11	128.7(2)	123.4(2)
O1−Cu2−Cl1	104.1(1)	106.00(4)	X1−Cu1−N11	123.0(2)	123.3(2)
O1−Cu2−Cl2	115.7(1)	100.68(4)	X2−Cu2−N21	130.8(2)	129.6(2)
			X1−Cu2−N21	118.4(2)	112.8(2)

[a] # [1] $-x+2, y+1/2, -z+1/2$; # [2] $x-1/2, -y+1/2, -z+2$.

The geometries of the non-linear copper units (Cu2) are distorted *pseudo* C_{3v} (**1a**) and D_{3h} (**1a′**). The oxygen atom (O1) occupies the vacant apical position in both structures. The Cu−O bond lengths in **1a** (2.472(3) Å) and **1a′** (2.375(1) Å) are above typical covalent bonds indicating a weak coordination of the oxygen to copper specially in **1a** also verified by angles Cl−Cu−O1 (**1a′**, 100.68(4), 106.00(4); **1a**, 104.1 (1), 115.7(1)) and N1−Cu2−O1 (**1a′**, 78.65(5); **1a**, 76.7(1)) (Table 1).

The conformational polymorphism of **1a′** and **1a** can be established by the torsion angles (Cu2−Cl−Cu1−O) defined by the planes Cu2,Cl,Cu1 and Cl,Cu1,O (**1a**, −15.90(7), 10.86(7)) and (**1a′**, −91.10(7), 49.51(7)) and the torsion angles Cu2−Cl2−Cu1−Cl1, Cl2−Cu1−Cl1−Cu2, Cu1−Cl1−Cu2−Cl2, and Cl1−Cu2−Cl2−Cu1 that display the values 130.32(6), 109.38(6), 160.94(6), 154.33(6) in **1a′** and −116.06(5), −41.72(5), 129.66(5), −141.40(5) in **1a**.

In the two polymorphic forms (**1a**, **1a′**) distinct orientations of the copper-chloride backbone (Figure 2) allow different torsion angles of the planes that contain the apical oxygen atom and the Cl−Cu−Cl backbone and permit different structural conformations. This possibility is due to the flexibility of the camphor hydrazone ligand ($YNC_{10}H_{14}O$) that renders more than one crystal lattice energetically accessible, which is essential to polymorphism.[7]

The two polymorphs also have different supramolecular arrangements although none of them displays classical hydrogen bonds. In **1a** weak intermolecular hydrogen bonds (C···Cl, H···Cl: 3.74(3), 2.90(5) Å, C−H···Cl 146.6(8)°) exist between the one-dimensional (1D) chains (Figure 3a) while in **1a′** no such type of interactions were

(7) Bernstein, J.; Davey, R. J.; Henck, J. O. *Angew. Chem., Int. Ed.* **1999**, *38*, 3441.

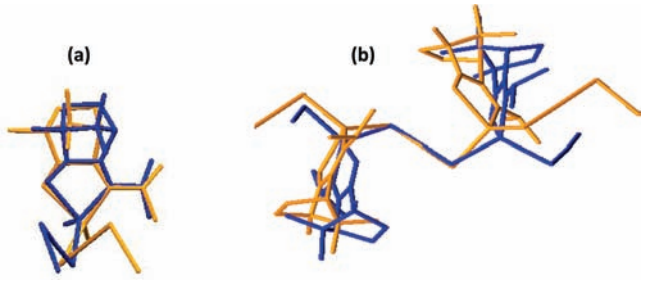

Figure 2. Overlay of one molecule (a) and backbone (b) of polymorphic forms of $[\{CuCl\}_2(Me_2NNC_{10}H_{14}O)]_n$ **1a′** (darker) and **1a** (lighter).

detected, instead intramolecular hydrogen interactions involving the oxygen (C···O, H···O: 3.38(4), 2.63(6)Å, 135.3(8)°) and the chloride atoms (C−H···Cl: 3.73(5), 2.92(6)Å, 141.3(8)°) are observed (Figure 3b). In **1a′** the supramolecular assembly promote an ABAB type of alternated "in phase" chains while in **1a** the sequential chains are "out of phase".

Several attempts to grow crystals from complexes $[\{CuX\}_2(YNC_{10}H_{14}O)]$ (Y = NHMe, **1b**; NH_2, **1c**) were unsuccessful. Thus, no comparative structural analysis in complexes with different Y groups is possible.

The only chain compound obtained from CuBr was $[\{CuBr\}_2(H_2NNC_{10}H_{14}O)]_n$ (**2c**)[1] in contrast with the complete set (**1a**, **1b**, **1c**) obtained from CuCl. This pattern suggests a better stabilization of the chain compounds $[\{CuX\}_2(YNC_{10}H_{14}O)]$ by chloride than by bromide. The steric non-demanding camphor hydrazone (Y = NH_2) is the only Y group able to overcome bromide steric hindrance or establish hydrogen bonding that stabilizes **2c**. Since no crystals of **2c** were obtained within the experimental work herein or before[1] structural characterization is missing. However, the surface properties (see below) compare well with those of **1a** (Table 2, 1 sweep).

A strict control of the copper halide and camphor hydrazone ratios (1:1) afforded compounds $[\{Cu(YNC_{10}H_{14}O)\}_2(\mu\text{-}X)_2]$ (X = Cl, Y = NMe_2 (**3a**), Y = NHMe (**3b**); X = Br, Y = NMe_2 (**4a**), Y = NHMe (**4b**)), reaction 11) except in the case of $H_2NNC_{10}H_{14}O$ that affords always $[\{CuX\}_2(H_2NNC_{10}H_{14}O)]_n$ (X = Cl or Br).

$$2CuX + 2YNC_{10}H_{14}O \rightarrow [\{Cu(YNC_{10}H_{14}O)\}_2(\mu\text{-}X)_2] \quad (\mathbf{3} \text{ or } \mathbf{4}) \qquad (1)$$

	X	Y
3a	Cl	NMe_2
3b	Cl	NHMe
4a	Br	NMe_2
4b	Br	NHMe

Compounds $[\{Cu(Me_2NNC_{10}H_{14}O)\}_2(\mu\text{-}Cl)_2]$ (**3a**) and $[\{Cu(Me_2NNC_{10}H_{14}O)\}_2(\mu\text{-}Br)_2]$ (**4a**) crystallize as dimers in the trigonal system ($P6_5$ space group, **3a** and $P6_1$ space group, **4a**) with the camphor ligands coordinated to copper through the oxygen and the imine nitrogen atoms. The copper atoms bridge through the halide (Figure 4) within short Cu−Cu distances (2.892(1) Å **3a**; 2.856(2) Å, **4a**). Selected bond lengths and angles are displayed in Table 1.

A peculiar characteristic of compounds **3a** (X = Cl) and **4a** (X = Br) is that the two coordinating nitrogen atoms occupy the same side of the molecule in contrast with opposite positions being found in structurally characterized Pd(II), Pt(II),[8−10] or Cu(II)[11] camphor derived complexes. Another observation is that the Cu−O bond lengths increase in the order **3a** < **1a′** < **1a** to values consistent with a low bidentate character of the camphor ligand in **1a**.

By addition of camphor dimethyl hydrazone to the chain compound $[\{CuCl\}_2(Me_2NNC_{10}H_{14}O)]$ (**1**) the dimer species $[\{Cu(Me_2NNC_{10}H_{14}O)\}_2(\mu\text{-}Cl)_2]$ (**3a**) forms (eq 2). The process can be reversed by reaction with CuCl (eq 3).

$$[\{CuCl\}_2(Me_2NNC_{10}H_{14}O)] + Me_2NNC_{10}H_{14}O \rightarrow [\{Cu(Me_2NNC_{10}H_{14}O)\}_2(\mu\text{-}Cl)_2] \qquad (2)$$

$$[\{Cu(Me_2NNC_{10}H_{14}O)\}_2(\mu\text{-}Cl)_2] + 2\ CuCl \rightarrow 2\ [\{CuCl\}_2(Me_2NNC_{10}H_{14}O)]_n \qquad (3)$$

1 → **3a** and **3a** → **1** conversion was confirmed by elemental analysis and infrared spectroscopy (Figure 5). A shift in the stretching frequencies of the C=O and C=N bonds of coordinated camphor dimethyl hydrazone (Figure 5) indicates that **1a** (ν_{CO} = 1701; ν_{CN} = 1550 converts to **3a** (ν_{CO}= 1681; ν_{CN} = 1540). In the reverse process the two polymorphic forms of $[\{CuCl\}_2(Me_2NNC_{10}H_{14}O)]$ were identified by IR (1691, **1a′**; 1701, **1a**, Figure 5b) but just crystals of **1a′** were suitable for X-ray diffraction analysis further corroborating preferential crystallization in form **1a′**.

To search for the structural aspects that favor polymer-dimer conversion a comparative analysis of the structures of the polymorphs (**1a** and **1a′**) and of the dimer (**3a**) was made. The results show that the torsion angles (Cu−Cl−Cu−O) calculated for **3a** (126.9(2), 139.0(2), 140.5(2), and 134.8(2)) are closer to the related calculated for **1a′** (−91.10(7), 49.51(7)) than for **1a** (−15.90(7), 10.86(7)) consequently the structural reorganization from **3a**→**1a′** or **1a′**→**3a** is easier. Crystallization in the polymorphic form **1a** would be expected since it does not convert easily in the dimer and also because of its two-dimensional (2D) character. However, that is not the case. Crystallization in form **1a′** generally occurs conceivably because of the viscosity of the solvent (tetrahydrofuran (THF)) that slows torsion relaxation toward **1a** and freezes the compound in the crystal form **1a′**.

Surface Study by XPS. In parallel with the study of the molecular characteristics and inter conversion of complexes $[\{CuX\}_2(YNNC_{10}H_{14}O)]_n$ and $[\{Cu(Me_2NNC_{10}H_{14}O)\}_2(\mu\text{-}X)_2]$ the characterization of the compounds was made by X-ray Photoelectron Spectroscopy (XPS). The technique was chosen because it provides information on the elemental composition of the surfaces and is sensitive to the oxidation state of the atoms. Therefore, it may elucidate the electron

(8) Carvalho, M. F. N. N.; Duarte, M. T.; Herrmann, R. *Collect. Czech. Chem. Commun.* **2006**, *71*(3), 302.
(9) Carvalho, M. F. N. N.; Galvão, A. M.; Ferreira, A. S. D. J. *Organomet. Chem.* **2009**, *694*, 2061.
(10) Carvalho, M. F. N. N.; Ferreira, A. S. D.; Ferreira da Silva, J. L.; Veiros, L. F. *Collect. Czech. Chem. Commun.* **2007**, *72*(5−6), 649.
(11) Carvalho, M. F. N. N.; Consiglieri, A. C.; Duarte, M. T.; Galvão, A. M.; Pombeiro, A. J. L.; Herrmann, R. *Inorg. Chem.* **1993**, *32*, 5160.

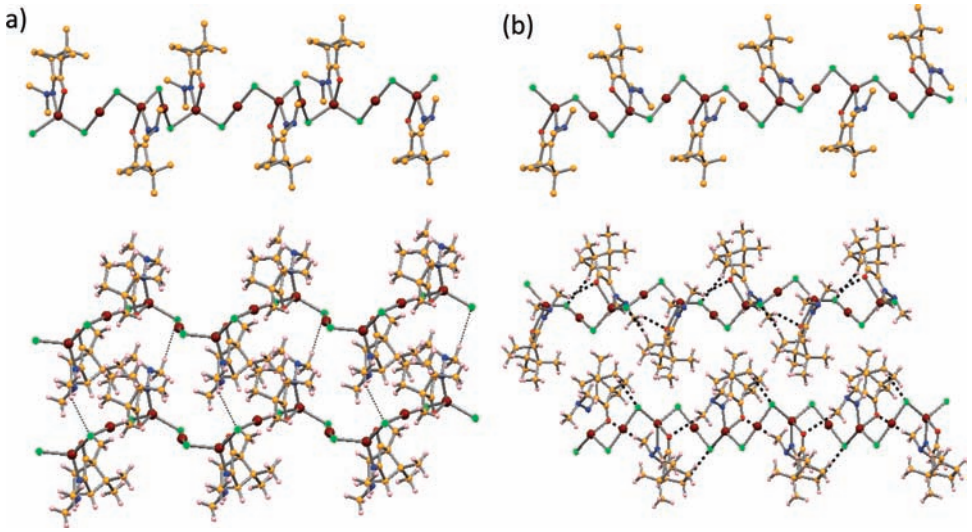

Figure 3. −(a) Supramolecular arrangement of **1a** (along c) showing the "in phase" chains. (b) View of the "out of phase" chains of **1a′** (along a).

Table 2. Atomic Ratios N/Cu and Cl/Cu for Cu(I) Complexes

		1a′[a]	**1a′**[a]	**1a**	**1c**	**2c**	**3a**	**4a**
	halogen	Cl	Cl	Cl	Cl	Br	Cl	Br
1 sweep	N/Cu	0.92	0.93	0.89	1.2	0.95	0.63	1.6
	deviation %	*7.8*	*7.2*	*12*	*22*	*5*	*69*	*20*
	Halide/Cu	1.1	1.1	0.85	1.0	1.1	1.1	0.98
	deviation %	*6.9*	*8.1*	*15*	*4*	*13*	*6*	*2*
5 sweeps	N/Cu	n.a.	0.66	0.64	1.2	0.90	0.36	1.7
	deviation %		*34*	*36*	*15*	*10*	*82*	*17*
	Halide/Cu	n.a	1.0	0.87	1.1	1.1	0.95	1.1
	deviation %		*0.1*	*13*	*6*	*13*	*5*	*11*
stoich	N/Cu	1	1	1	1	1	2	2
	Halide/Cu	1	1	1	1	1	1	1

[a] Samples obtained from different batches for comparative purposes.

distribution around the copper, chloride, and nitrogen atoms and provide information on stability and reactivity trends.

A representative selection of the coordination polymers (**1a**, **1a′**, **1b**, **1c**, **2c**) and dimers (**3a** and **4a**) was studied by XPS.

Detailed XPS regions for Cu 2p, Cl 2p, Br 2p, and N 1s (Figure 6) as well as for C 1s and O 1s regions and survey spectra (not shown here) were acquired for all compounds. The C 1s and O 1s regions are not discussed because they contain significant contributions of the sample holder, as deduced from XPS C/Cu and O/Cu atomic ratios.

For all samples, except **3a**, the Cu 2p region displays a doublet with an spin-orbit split of 19.8 eV with the component $2p_{3/2}$ centered at 932.8 ± 0.3 eV which is a value typical of copper in halide (Cl or Br) complexes.[12] In **3a** the quality of the peak fitting clearly improves when a second peak (more than 10 times weaker than the main one) centered at 935.2 ± 0.2 eV is added. This peak is usually assigned to Cu(II) species bound to hydroxyl groups.[13] The presence of Cu(II) is also revealed by multiplet structures in the region 939−945 eV[14] which are identified as incipient signals in the chloride dimer (**3a**) (Figure 6a) but are absent in **1a**, **1a′**, **1b**, **1c**, and **4a** indicating that in these cases just Cu(I) exists. The presence of Cu(II) in sample **3a** is likely a product of degradation induced by X-ray radiation.

The Cu Auger parameter is a sounder parameter for identification of the oxidation state of a metal since it is not affected by shifts caused by charge accumulation. Cu $2p_{3/2},L_3M_{45}M_{45}$ was found to be 1847.3 ± 0.2 eV for all the samples in agreement with values published for other polynuclear copper chloride compounds[12] and close to values found for Cu(I) compounds. It is, nevertheless, worthy to notice that the full width at half-maximum (fwhm) is not uniform: samples **1c** and **2c** present fwhm = 1.60 ± 0.05 eV whereas all the other samples display fwhm = 2.0 ± 0.1 eV.

The differences in fwhm are, in principle, due to unimodal (the narrow ones) or multimodal (the broader ones) electronic densities on Cu atoms. This means that Cu atoms in samples of type **c** (Y = NH_2) have an electronic density much more uniform than in samples of type **a** (Y = NMe_2). Extended hydrogen bridging in compounds **1c** and **2c** may account for a more rigid structure that precludes dimer complexes to form.

Cl 2p region is also a doublet with the components $2p_{3/2}$ and $2p_{1/2}$ separated by 1.6 eV and the main component Cl $2p_{3/2}$ centered at 198.9 ± 0.2 eV which is exactly the value found for dichloro(tetraphenylphosphonium)-copper.[15] However, just compound **3c** is well fitted with a single doublet (Figure 5b) each component having fwhm = 1.35 eV, the narrowest ones as observed also for Cu 2p peaks. All the other compounds display broader doublets (fwhm = 1.5 to 1.7 eV) and can be fitted with a second doublet. The component $2p_{3/2}$ of the second doublet is centered at 199.8 ± 0.2 eV for the sample **1a**, and its intensity has the same order of magnitude as the other Cl $2p_{3/2}$ peak. This component is assigned to a

(12) Wagner, C. D.; Naumkin, A. V.; Kraut-Vass, A.; Allison, J. W.; Powell, C. J.; Rumble, J. R.; Jr. NIST X-ray Photoelectron Spectroscopy Database, NIST, Standard Reference Database 20, Version 3.4 (Web Version) (2003). http://srdata.nist.gov/xps/ (accessed in 2010).

(13) Marques, M. T.; Ferraria, A. M.; Correia, J. B.; Botelho do Rego, A. M.; Vilar, R. *Mater. Chem. Phys.* **2008**, *109*, 174.

(14) Battistoni, C.; Mattongno, G.; Paparazzo, E.; Naldini, L. *Inorg. Chim. Acta* **1985**, *102*, 1.

(15) Folkesson, B.; Sundberg, P.; Johansson, L.; Larsson, R. J. *Electron Spectrosc. Relat. Phenom.* **1983**, *32*, 245.

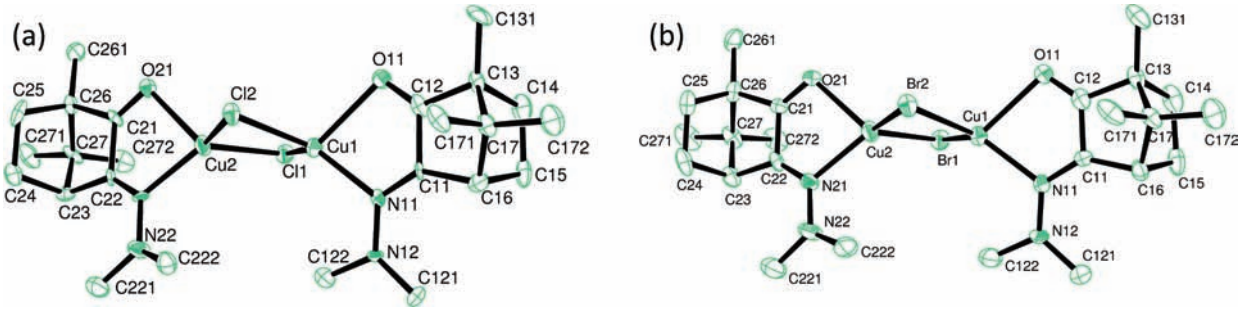

Figure 4. ORTEP drawing showing labeling scheme for (a) [{Cu($Me_2NNC_{10}H_{14}O$)}$_2$(μ-Cl)$_2$] (**3a**) and (b) [{Cu($Me_2NNC_{10}H_{14}O$)}$_2$(μ-Br)$_2$] (**4a**).

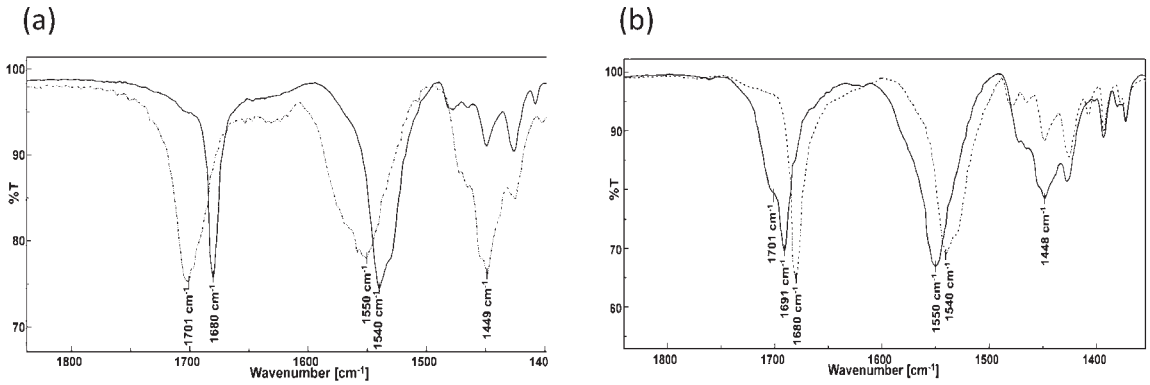

Figure 5. IR spectra of [{CuCl}$_2$($Me_2NNC_{10}H_{14}O$)] (dotted lines, **1a**) and [{Cu($Me_2NNC_{10}H_{14}O$)}$_2$(μ-Cl)$_2$] (solid lines, **3a**) showing conversions: (a) **1a**→ **3a**; (b) **3a**→ **1** (**a**′+ **a**).

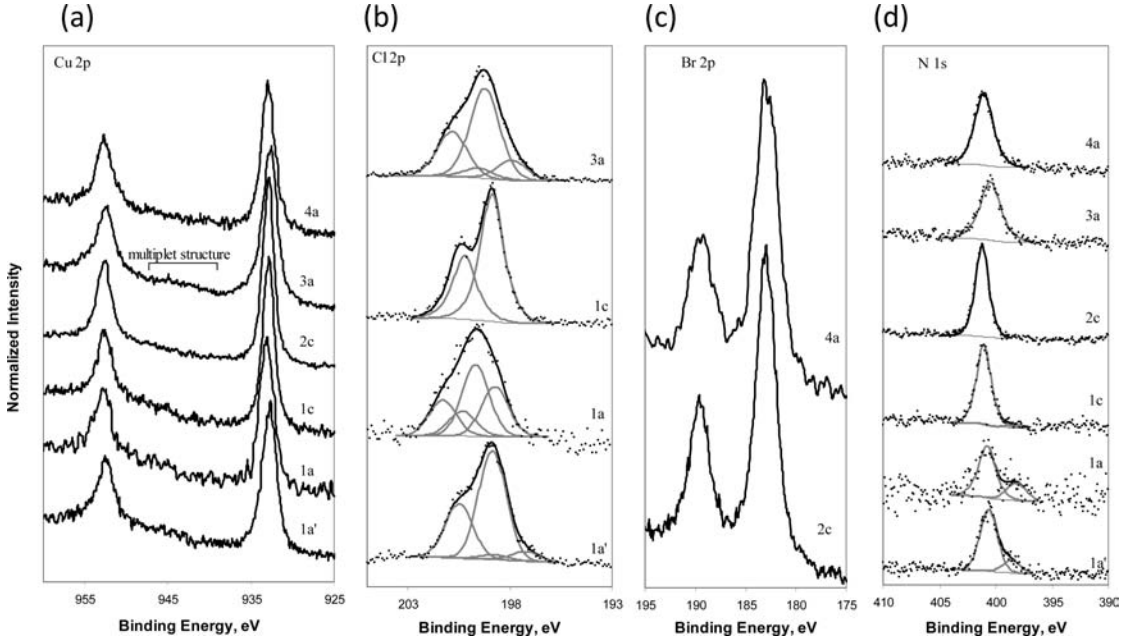

Figure 6. XPS data obtained for all the samples in the regions Cu 2p (a), Cl 2p (b), Br 2p (c), and N 1s (d). All the spectra in each region were normalized to equal area. Spectra were displaced vertically for sake of clarity.

chloride atom weakly bound to copper in excellent agreement with the long Cu−Cl bond length (2.333 Å) measured by X-ray diffraction analysis (Table 1). In the other two samples, **1a**′ and **3a**, the second doublet has a much smaller area than the main one, and its $2p_{3/2}$ component is displaced toward lower binding energy. Degradation of the sample induced by X-ray radiation may account for this small component.

The Br 2p region (figure 6c) also shows a doublet with a separation of 6.5 eV and the component $2p_{3/2}$ centered at 182.4 ± 0.2 eV which is close to the value reported for dibromo(tetraphenylphosphonium)copper.[10] In samples **2c** and **4a**, a single doublet is enough to fit the spectra. However, such as observed for Cu 2p, sample **2c** displays narrower peaks (fwhm = 2.35 ± 0.05 eV) than sample **4a** (fwhm = 2.8 ± 0.1 eV).

In the N 1s region (Figure 6d) XPS signals are fittable with a single component although, two signals of similar intensity would be expected if the imine and the amine nitrogen atoms at complexes $[\{CuX\}_2L]_n$ and $[\{CuXL\}_2]$ ($L = YNC_{10}H_{14}O$; $Y = NMe_2$, NHMe, or NH_2) were distinct. The value measured that is centered at 400.8 ± 0.3 eV is higher than the usual values (399 to 400 eV[16]) for N bound to C and/or H in agreement with nitrogen acting as electron donor to copper. It is noteworthy that in samples **1a** and **1a′**, a second nitrogen component is detected at lower energy (398.5 ± 0.3 eV) which increases with time irradiation. This second peak is assigned to a species resulting from sample degradation.

From the quantitative point of view, atomic ratios N/Cu and halide/Cu were computed and are shown in Table 2. Atomic ratios involving carbon will not be included, since carbon exists in the sample holder and in residues of solvents incompletely removed.

Table 2 displays atomic ratios for different times of acquisition: 1 sweep, followed by 5 sweeps (irradiation time 5 times longer) *per* region to search for degradation of the compounds induced by X-radiation. Halogens bound to carbon are known to be very labile under X-radiation,[17,18] thus the upper procedure was adopted to check for halogen loss during irradiation. Results have shown that, within estimated experimental error (≤15%), all the atomic ratios halogen/copper have the expected stoichiometric value. However, in what concerns the ratio N/Cu there are deviations from the stoichiometric values that in some samples are far beyond the estimated experimental error. Deviations are negative (N/C*u* < 1) indicating nitrogen loss during XPS measurements except in the case of compound **1c** (1.22). Additionally, the N/Cu ratios decrease with increasing time of irradiation. This trend is more pronounced in chloride than bromide complexes (Table 2). The extreme values were measured in the chloride dimer $[\{Cu(Me_2NNC_{10}H_{14}O)\}_2(\mu\text{-}Cl)_2]$ (**3a**) that after just one sweep displays a N/Cu ratio around 30% of the expected value (0.63 instead of 2) and still decreases after five sweeps (0.36; Table 2). Such trend indicates that XPS radiation promotes degradation of the sample. However, since a single N 1s peak is detected, the product of degradation leaves the sample which is under ultrahigh vacuum. Ligand loss ($YNC_{10}H_{14}O$) promoted by heating associated to XPS radiation may account for the observed low N/Cu values, since complete decomposition to ligand ($Me_2NNC_{10}H_{14}O$) *plus* CuCl was confirmed by heating $[\{Cu(Me_2NNC_{10}H_{14}O)\}_2(\mu\text{-}Cl)_2]$ ($T = 100$ °C, $P = 5 \times 10^{-3}$ bar).

Conclusions

The coordination polymer $[\{CuCl\}_2(Me_2NNC_{10}H_{14}O)]_n$ exists in two polymorphic forms that differ essentially in Cu−Cl−Cu−O torsions angles and hydrogen interactions. The *in phase* polymorph (**1a**) displays non-conventional hydrogen bonds between layers (some 2D character) while the *out of phase* polymorph (**1a′**) displays no such type of interlayer interactions, instead intramolecular hydrogen bridges exist. Both polymorphs convert to the dimer $[\{Cu(Me_2NNC_{10}H_{14}O)\}_2(\mu\text{-}Cl)_2]$ by reaction with dimethyl hydrazone. The reaction can be reversed by addition of CuCl. The structure of the polymorph **1a′** favors the process.

The dimer−polymer conversions are better promoted in chloride (**3**) than in bromide (**4**) compounds. This reactivity pattern was also detected during XPS measurements through faster nitrogen loss in **3a** than in **4a** that is consistent with the higher lability of the camphor hydrazone ligand in chloride than in bromide compounds. XPS studies also give a clue on no dimer hydrazono ($Y = NH_2$) formation based on the highly uniform electronic density in $[\{CuX\}_2(H_2NNC_{10}H_{14}O)]$ (X = Cl or Br) due to extended hydrogen bridging that stabilizes the polymers.

Experimental Section

All complexes were prepared under inert atmosphere using vacuum and Schlenk techniques. Camphor derived[19,20] as well as the chain compounds $[\{CuCl\}_2(YNC_{10}H_{14}O)]_n$ ($Y = NMe_2$, NHMe, NH_2)[1] were prepared by published methods. CuCl was synthesized from $CuCl_2$ by reduction with sodium sulphite.[21] CuBr was purchased from Fluka. Solvents were purchased from Sigma-Aldrich purified by conventional techniques and distilled before use. IR spectra were obtained in a JASCO FT/IR 4100 spectrometer. NMR spectra (^1H, ^{13}C, DEPT, HSQC HMBC) were obtained in DMSO-d_6 using Bruker Avance II$^+$ Spectrometers (300 or 400 MHz). TMS ($\delta = 0$ ppm) was used as internal reference. The numbering scheme is shown below.

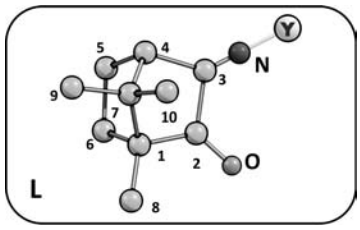

XPS Analysis. For X-ray photoelectron spectroscopy (XPS) studies, samples were mounted on the sample stub using a double-sided tape. Samples were analyzed using a XSAM800 (Kratos) X-ray spectrometer operated in the fixed analyzer transmission (FAT) mode, with a pass energy of 20 eV, a power of 120 W, and the unmonochromatized Al Kα X-radiation ($h\nu = 1486.6$ eV). Typical base pressure in the ultrahigh vacuum (UHV) analysis chamber was in the range of 10^{-7} Pa. All sample transfers were made in air. Samples were analyzed at room temperature, at a takeoff angle of 45° relative to the normal of the surface, as usual in powdered samples.[22] Spectra were collected and stored in 300 channels with a step of 0.1 eV using a Sun SPARC Station 4 and with Vision software (Kratos). The curve fitting for component peaks was carried out with a non-linear least-squares algorithm using a product of Gaussian and Lorentzian peak shapes (pseudo Voigt profiles) and Shirley background. The XPSPeak41 freeware at the WEB[23] was used. No flood gun was used for charge

(16) Beamson, G.; Briggs, D. *High Resolution XPS of Organic Polymers: The Scienta ESCA300 Database*; John Wiley & Sons: New York, 1992.
(17) Ferraria, A. M.; Lopes da Silva, J. D.; Botelho do Rego, A. M. *Polymer* **2003**, *44*(23), 7241–7249.
(18) Pimentel Real, L. E.; Ferraria, A. M.; Botelho do Rego, A. M. *Polym. Test*. **2007**, *26*, 77.
(19) Carvalho, M. F. N. N.; Costa, L. M. G.; Pombeiro, A. J. L.; Schier, A.; Scherer, W.; Harbi, S. K.; Verfürth, U.; Herrmann, R. Z. *Naturforsch*. **1994**, *33b*, 6270.
(20) Santos, A. M.; Carvalho, M. F. N. N.; Galvão, A. M.; Pombeiro, A. J. L. *Z. Naturforsch*. **2002**, *57b*, 691–8.
(21) Tanaka, J.; Suib, S. L. *Experimental Methods in Inorganic Chemistry*; Prentice Hall, Inc.: London, U.K., 1999; p 231.
(22) Garbout, A.; Bouattour, S.; Botelho do Rego, A. M.; Ferraria, A. M.; Kolsi, A. W. *J. Cryst. Growth* **2007**, *304*(2), 374–382.
(23) http://www.wsu.edu/~scudiero/, accessed in 2009.

Table 3. Crystallographic Data for $[(CuCl)_2(Me_2NNC_{10}H_{14}O)]_n$ Obtained at 150 K

	$[(CuCl)_2(Me_2NN-C_{10}H_{14}O)]_n$ (**1a**)	$[(CuCl)_2(Me_2NNC_{10}-H_{14}O)]_n$ (**1a′**)
empirical formula	$C_{12}H_{20}N_2OCl_2Cu_2$	$C_{12}H_{20}N_2OCl_2Cu_2$
formula weight	406.28	406.3
temperature (K)	150	150
wavelength	0.71073	0.71073
crystal system	monoclinic	orthorhombic
space group	$P2_1$	$P2_12_12_1$
unit cell dimensions		
a/ Å	7.438(3)	7.9928(4)
b/ Å	10.841(4)	11.2136(6)
c/ Å	10.050(4)	17.3838(8)
α/ deg	90	90
β/ deg	98.52(1)	90
γ/ deg	90	90
volume (Å^{-3})	801.5(5)	1558.1(1)
Z	2	4
D_{cal} (g/cm^3)	1.684	1.732
absorption coefficient (mm^{-1})	2.979	3.065
F(000)	412	824
crystal size (mm^3)	0.2 × 0.3 × 0.2	0.3 × 0.3 × 0.2
θ range for data collection (deg)	2.77 to 31.30	2.80 to 31.37
index ranges	$-9 \le h \le 10$ $-9 \le k \le 15$ $-14 \le l \le 11$	$-11 \le h \le 11$ $-16 \le k \le 14$ $-25 \le l \le 25$
refinement method	full-matrix least-squares on F^2	full-matrix least-squares on F^2
data/restraints/parameters	4082/1/172	5138/0/177
final R (observed)	R1 = 0.0347, wR2 = 0.0726	R1 = 0.0248, wR2 = 0.0553

compensation. For charge shifts due to the insulating character of samples, sp^3 carbon bound to carbon and hydrogen was used as reference taking Binding Energy (C 1s) = 285 eV. For quantification purposes, the following sensitivity factors were used: N 1s, 0.42; Cl 2p, 0.73; and Cu $2p_{3/2}$, 4.2.

X-ray Diffraction Analysis. X-ray diffraction analysis was performed on a red crystal of $[\{CuCl\}_2(Me_2NNC_{10}H_{14}O)]$ (**1a**) and $[\{Cu(Me_2NNC_{10}H_{14}O)\}_2(\mu\text{-}Br)_2]$ (**4a**). Data was collected on a Bruker AXS-KAPPA APEX II area detector apparatus using graphite-monochromated Mo Kα ($\lambda = 0.71073$ Å) and were corrected for Lorentz, polarization, and empirically for absorption effects. Cell dimensions were determined from the setting angles of reflections 4082 for (**1a**), 5138 for (**1a′**), 3302 for (**3a**), and 4058 for (**4a**). Complex **1a** crystallizes in the monoclinic space group $P21$ and complex **4a** in the trigonal space group $P61$. The structures were solved by direct methods using SHELX97[24] and refined by full matrix least-squares against F^2 using SHELX97, all included in the suite of programs WinGX v1.70.01 for Windows.[25] Non-hydrogen atoms were refined anisotropically, and H atoms were inserted in idealized positions and allowed to refine riding on the parent carbon atom.

Crystal data and refinement parameters are summarized in Tables 3 and 4. Illustrations of the molecular structures were made with ORTEP3.[26]

CCDC xxxxxx contains the supplementary crystallographic data for this paper.

The X-ray data can be obtained free of charge via www.ccdc.cam.ac.uk/conts/retrieving.html (or from the Cambridge Crystallographic Data Centre, 12, Union Road, Cambridge, CB2 1EZ, U.K.; fax: +44 1223 336033; or deposit@ccdc.cam.ac.uk).

(24) Sheldrick, G. M. *SHELX-97- Programs for Crystal Structure Analysis* (release 97-2); Institüt für Anorganische Chemie der Universität: Göttingen, Germany, 1998.
(25) *WINGX*; Farrugia, L. J. *J. Appl. Crystallogr.* **1999**, *32*, 837.
(26) Farrugia, L. J. *J. Appl. Crystallogr.* **1997**, *30*, 565.

Table 4. Crystallographic Data $[\{Cu(Me_2NNC_{10}H_{14}O)\}_2(\mu\text{-}X)_2]$ (X = Cl or Br) Obtained at 150 K

	$[\{Cu(Me_2NNC_{10}-H_{14}O)\}_2(\mu\text{-}Cl)_2]$ (**3a**)	$[\{Cu(Me_2NNC_{10}H_{14}-O)\}_2(\mu\text{-}Br)_2]$ (**4a**)
empirical formula	$C_{24}H_{40}N_4O_2Cl_2Cu_2$	$C_{24}H_{40}N_4O_2Br_2Cu_2$
formula weight	614.58	703.50
temperature (K)	150	150
wavelength	0.71073 A	0.71073 A
crystal system	trigonal	trigonal
space group	$P6_1$	$P6_1$
unit cell dimensions		
a/Å	10.4748(7)	10.569(2)
b/Å	10.4748(7)	10.569(2)
c/Å	42.000(3)	42.77(1)
α/ deg	90	90
β/ deg	90	90
γ/ deg	120	120
volume (Å^{-3})	3990.9(5)	4138(2)
Z	6	6
D_{cal} (g/cm^3)	1.534	1.694
Absorption coefficient (mm^{-1})	1.828	4.467
F(000)	1920	2136
crystal size (mm^3)	0.3 × 0.1 × 0.1	0.1 × 0.2 × 0.1
θ range for data collection (deg)	2.25 to 22.09	2.22 to 23.49
index ranges	$-1 \le h \le 11$ $-1 \le k \le 10$ $-44 \le l \le 44$	$-1 \le h \le 11$ $-1 \le k \le 11$ $-47 \le l \le 47$
refinement method	full-matrix least-squares on F^2	full-matrix least-squares on F^2
data/restraints/ parameters	3302/1/311	4058/1/312
final R (observed)	0.0379, wR2 = 0.0708	0.0352, wR2 = 0.0806

Synthesis. Complexes $[\{Cu(Me_2NNC_{10}H_{14}O)\}_2(\mu\text{-}X)_2]$ (X = Cl or Br; Y = NMe_2, NHMe) were obtained from the corresponding copper halide by reaction with the appropriate camphor hydrazone ($YNC_{10}H_{14}O$). Typically equimolar amounts or a slight excess (ca. 10%) of $YNC_{10}H_{14}O$ and CuX were mixed in THF (ca. 2−5 cm^3) and stirred for 2−4 h.

$[\{Cu(Me_2NNC_{10}H_{14}O)\}_2(\mu\text{-}Cl)_2]$ (3a). (*E*)-3-(2,2-Dimetil-hidrazono-1,7,7-trimethyl-bicyclo[2.2.1] heptan-2-one (0.103 g, 0.50 mmol) and CuCl (0.049 g, 0.49 mmol) were stirred in THF (2 cm^3) for 3 h. Addition of *n*-pentane (2 cm^3) to the filtered solution affords the complex (0.12 g, 0.39 mmol). Yield 80%. Elemental analysis (%) for $CuC_{12}H_{20}ClN_2O$: Found: C 46.8, N 9.0, H 6.6. Calculated: C 46.9, N 9.1, H 6.5. IR (cm^{-1}): 1681 (υ_{CO}), 1539 (υ_{CN}). ^{1}H NMR (DMSO, δ ppm): 3.14 (d, J_{HH} = 4.0, 1H), 3.05 (s, 6H), 2.00−1.17 (m, 4H), 0.90 (s, 3H), 0.86 (s, 3H), 0.76 (s, 3H). ^{13}C NMR (DMSO, δ ppm): 203.6, 142.2, 55.8, 49.8, 45.7, 45.4, 29.4, 25.6, 20.3, 17.9, 9.3.

$[\{Cu(MeHNNC_{10}H_{14}O)\}_2(\mu\text{-}Cl)_2]$ (3b). (*E*)-3-(2,2-Metil-hidrazono-1,7,7-trimethyl-bicyclo[2.2.1] heptan-2-one (0.082 g, 0.42 mmol) and CuCl (0.042 g, 0.42 mmol) were stirred in THF (1 cm^3) for 4 h. The title complex was obtained as a yellow solid (0.030 g, 0.10 mmol; yield 24%.) upon filtration. Elemental analysis (%) for $CuC_{11}H_{18}ClN_2O\cdot 1/2H_2O$: Found: C 44.1, N 8.9, H 6.2. Calculated: C 44.4, N 9.4, H 6.2. IR (cm^{-1}): 3310 (υ_{NH}), 1695 (υ_{CO}), 1577 (υ_{CN}). ^{1}H NMR (DMSO, δ ppm): 7.6(s_{br}, 1H), 3.0 (s, 3H), 2.89 (s_{br}, 1H), 1.90−1.28 (m, 4H), 0.91 (s, 3H), 0.86 (s, 3H), 0.73 (s, 3H). ^{13}C NMR (DMSO, δ ppm): 202.8, 143.5, 57.2, 45.3, 37.1, 31.0, 23.5, 20.0, 17.9, 9.1.

$[\{Cu(Me_2NNC_{10}H_{14}O)\}_2(\mu\text{-}Br)_2]$ (4a). (*E*)-3-(2,2-Dimetil-hidrazono-1,7,7-trimethyl-bicyclo[2.2.1] heptan-2-one (0.12 g, 0.58 mmol) *plus* CuBr (0.085 g, 0.59 mmol) were mixed and stirred in THF (2 cm^3) for 3 h. Addition of *n*-pentane (2 cm^3) to the filtered solution afforded a red complex. A further crop was obtained from the solution by addition of pentane (total: 0.11 g, 0.33 mmol; yield

57%). Elemental analysis (%) for $CuBrC_{12}H_{20}N_2O$: Found: C 41.5, N 7.9, H 5.9. Calculated: C 41.0, N 8.0, H 5.7. IR (cm^{-1}): 1691 (υ_{CO}), 1550 (υ_{CN}). ^1H NMR (DMSO, δ ppm): 3.14 (d, J_{HH} = 4.4, 1H), 3.05 (s, 6H), 2.00−1.27 (m, 4H), 0.90 (s, 3H), 0.86 (s, 3H), 0.76 (s, 3H). ^{13}C NMR (DMSO, δ ppm): 203.5, 142.1, 55.8, 49.8, 45.6, 45.3, 29.4, 25.5, 20.3, 17.8, 9.2.

[{Cu(MeHNNC$_{10}$H$_{14}$O)}$_2$(μ-Br)$_2$] (4b). (*E*)-3-(2-Metil-hidrazono-1,7,7-trimethyl-bicyclo[2.2.1] heptan-2-one (0.135 g, 0.69 mmol) *plus* CuBr (0.95 g, 0.66 mmol) were mixed and stirred in THF (4 cm^3) for 3 h. Addition of *n*-pentane (3 cm^3) to the filtered solution afforded a dark orange compound (0.030 g, 0.090 mmol; yield 14%). Elemental analysis (%) for $CuBrC_{12}H_{20}N_2O \cdot 1/5\ C_5H_{12}$. Found: C 41.1, N 8.4, H 6.1. Calculated: C 40.9, N 8.0, H 5.8. IR (cm^{-1}): 1702 (υ_{CO}), 1578 (υ_{CN}). ^1H NMR (DMSO, δ ppm): 7.51 (s, 1H), 3.40 (s, 3H), 2.98 (d, J_{HH} = 3.6, 1H) 1.89−1.27 (m, 4H), 0.90 (s, 3H), 0.85 (s, 3H), 0.73 (s, 3H). ^{13}C NMR (DMSO, δ ppm): 202.7, 143.1, 57.2, 45.2, 45.1, 37.0, 31.0, 23.6, 20.0, 18.0, 9.2.

Acknowledgment. To Fundação para a Ciência e Tecnologia (FCT) for financial support to Project PPCDT 58119/QUI/2004 and a Ph.D. grant to T.A.F. (SFRH/BD/48331/2008).